



## **Circulator Load Modulated Amplifier: A Non-Reciprocal Wideband and Efficient PA Architecture**

Downloaded from: <https://research.chalmers.se>, 2025-06-18 04:11 UTC

Citation for the original published paper (version of record):

Zhou, H., Perez-Cisneros, J., Fager, C. (2021). Circulator Load Modulated Amplifier: A Non-Reciprocal Wideband and Efficient PA Architecture. IEEE MTT-S International Microwave Symposium Digest, 2021-June: 603-605. <http://dx.doi.org/10.1109/IMS19712.2021.9574960>

N.B. When citing this work, cite the original published paper.

© 2021 IEEE. Personal use of this material is permitted. Permission from IEEE must be obtained for all other uses, in any current or future media, including reprinting/republishing this material for advertising or promotional purposes, or reuse of any copyrighted component of this work in other works.

As it can be seen in Fig. 1, the main and auxiliary amplifiers are connected to the circulator at ports P1 and P3, respectively. They have different amplitudes  $I_m$  and  $I_a$ , respectively, with a phase offset  $\theta$  between them. Thus,  $I_1 = -I_m$ ,  $I_3 = -I_a e^{j\theta}$ . The output port (P2) is terminated with a resistive load equal to the characteristic impedance of the circulator,  $Z_0$ . Therefore,  $V_2 = -Z_0 I_2$ .

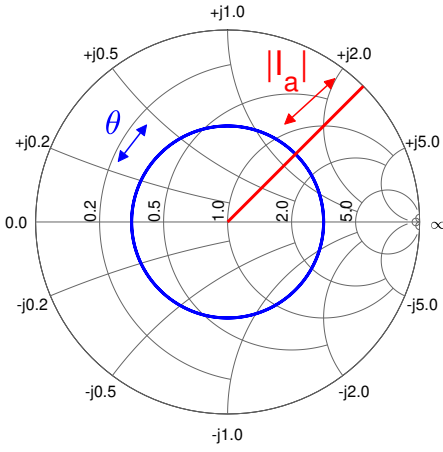


Fig. 2. Effect of auxiliary signal amplitude and phase variation on the impedance seen by the main amplifier of the CLMA architecture.

Substituting the above equations into the 3-port admittance matrix, the resulting set of equations can be solved to obtain the expression for the impedances seen by the main amplifier, denoted as  $Z_m$ , as follows

$$Z_m = Z_0(1 + 2\frac{I_a e^{j\theta}}{I_m}). \quad (2)$$

Eq. (2) reveals that the impedance seen by the main amplifier can be dynamically modulated by varying the magnitude and phase of the auxiliary current. Fig. 2 shows the effect of signal amplitude and phase from the auxiliary amplifier on the impedance seen by the main amplifier.

Moreover, from the set of equations above, the relationship between the currents can be determined by

$$I_2 = I_m + I_a e^{j\theta}. \quad (3)$$

Furthermore, it can be verified that  $P_2 = P_m + P_a$ , which proves that the power injected by the main and auxiliary amplifiers is fully transferred to the output port. For simplicity, mathematical derivations are skipped.

According to the theory, it is possible to present the optimal impedance to the main amplifier at different output power levels by properly controlling the magnitude and phase of the auxiliary amplifier current. In addition, the power of both constituting amplifiers is delivered to the load. Hence, the CLMA architecture is capable of maintaining high efficiency over a large output power range. In principle, the bandwidth is limited only by the 3-port non-reciprocal output combiner.

It should be remarked that the impedance seen by the auxiliary amplifier is maintained constant, and equal to  $Z_0$ , due to the high isolation from main to auxiliary ports. Moreover, the main amplifier only needs to be matched to provide high efficiency at a single power level across the considered bandwidth. Therefore, the design requirements of the output matching networks of the constituting amplifiers of the CLMA are considerably relaxed compared to other load modulating architectures.

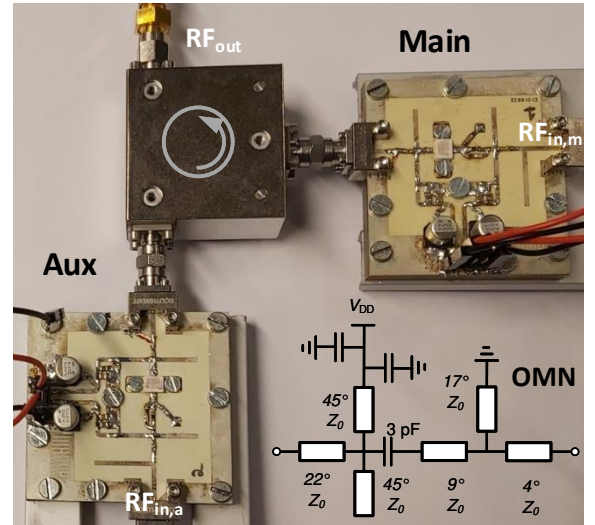


Fig. 3. Photograph of the CLMA demonstrator including detailed schematic of the OMN.

### III. EXPERIMENTAL VERIFICATION

As a proof of concept, a demonstrator is employed to validate the CLMA approach. It is based on GaN transistors and a commercial circulator.

A PA test board based on a 10-W GaN HEMT CGH40010F packaged transistor from Wolfspeed is used to perform as both main and auxiliary amplifiers. The output matching network (OMN) of the PA test board was designed following a strategy for the maximization of back-off efficiency at 2.14 GHz.

The three-port SM2040C09 circulator from Quest Microwave is selected to act as the output combiner since it has both low insertion loss and high isolation.

Fig. 3 shows a photo of the CLMA demonstrator together with a detailed schematic of the OMN. In addition, a 3dB-Wilkinson power splitter and a phase shifter in the auxiliary amplifier branch were employed to characterize the CLMA in order to evaluate its performance.

The CLMA demonstrator has been characterized with static CW measurements. The drain bias of the main and auxiliary amplifiers were set to 28 V and 34 V, respectively. The main amplifier was biased in class-B (25 mA quiescent current) whilst the auxiliary amplifier was biased in class-C ( $V_{GS} = -6V$ ). A input power splitting ratio of approximately 50% has been employed. The optimum phase delay for 1.99, 2.04, 2.09 and 2.14 GHz has been selected.

Fig. 4 shows the measured drain efficiency versus output power profiles for several frequencies. It exhibits of  $43.3 \pm 0.4$  dBm and drain efficiency of 73.2-58% at 6-dB output power control range across 2.04-2.14 GHz. At 2.09 GHz, drain efficiency figures of 73%/48% were measured over 6/10 dB of output power control range, respectively. Table I compares these results with those from representative state-of-the-art load modulated PAs.

### IV. CONCLUSION

A novel PA architecture based on a 3-port non-reciprocal combiner network has been proposed and verified. The use of

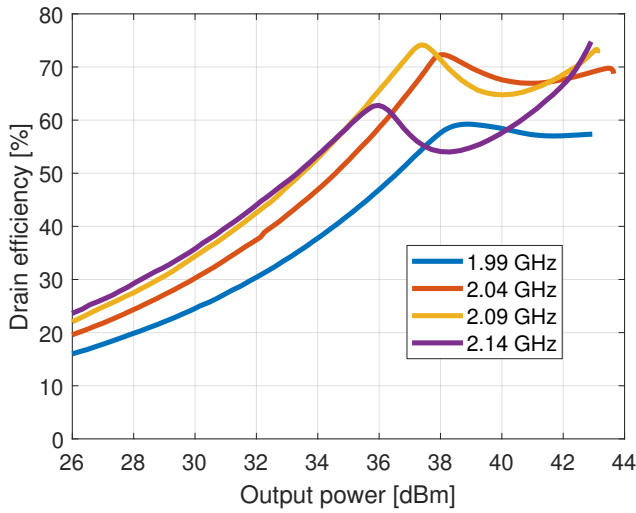


Fig. 4. Measured drain efficiency versus output power profiles at different frequencies.

Table 1. Comparison with state-of-the-art load modulated PAs.

| Reference        | Topology    | Freq (GHz)  | $P_{\max}$ (dBm) | $\eta_{6\text{dB}/10\text{dB}}$ (%) |
|------------------|-------------|-------------|------------------|-------------------------------------|
| [8]              | Outphasing  | 0.7         | 47.4             | 80/70                               |
| [9]              | Doherty     | 1.95        | 44               | 62/52                               |
| [10]             | Outphasing  | 2.3         | 48.5             | 60/55                               |
| [11]             | LMBA        | 2.4         | 45.6             | 54/38                               |
| [12]             | Doherty     | 3.5         | 44.5             | 68/52                               |
| <b>This work</b> | <b>CLMA</b> | <b>2.09</b> | <b>43.1</b>      | <b>73/48</b>                        |

a non-reciprocal combiner reduces the interaction between the main- and auxiliary branches, which simplifies the design of the amplifiers. Combined with the availability of broadband low-loss circulators, it has the potential to provide broadband highly-efficient operation over large output power control range. As a first validation of the new PA architecture a narrowband high performance demonstrator has been realized.

#### ACKNOWLEDGMENT

This research has been carried out in the GigaHertz Centre in a joint project financed by the Swedish Government Agency for Innovation Systems (VINNOVA), Chalmers University of Technology, Ericsson, Gotmic, Infineon Technologies Austria, Qamcom, RISE, and SAAB.

#### REFERENCES

- [1] F. H. Raab, P. Asbeck, S. Cripps, P. B. Kenington, Z. B. Popovic, N. Potheary, J. F. Sevic, and N. O. Sokal, "Power amplifiers and transmitters for RF and microwave," *IEEE Transactions on Microwave Theory and Techniques*, vol. 50, no. 3, pp. 814–826, 2002.
- [2] P. Asbeck and Z. Popovic, "ET Comes of Age: Envelope Tracking for Higher-Efficiency Power Amplifiers," *IEEE Microwave Magazine*, vol. 17, no. 3, pp. 16–25, 2016.
- [3] W. H. Doherty, "A New High Efficiency Power Amplifier for Modulated Waves," *Proceedings of the Institute of Radio Engineers*, vol. 24, no. 9, pp. 1163–1182, 1936.
- [4] H. Chireix, "High power outphasing modulation," *Proceedings of the Institute of Radio Engineers*, vol. 23, no. 11, pp. 1370–1392, 1935.
- [5] G. Nikandish, R. B. Staszewski, and A. Zhu, "Breaking the bandwidth limit: A review of broadband doherty power amplifier design for 5g," *IEEE Microwave Magazine*, vol. 21, no. 4, pp. 57–75, 2020.

- [6] R. A. Beltran, "Broadband outphasing transmitter using class-e power amplifiers," in *2019 IEEE MTT-S International Microwave Symposium (IMS)*, 2019, pp. 67–70.
- [7] D. J. Sheppard, J. Powell, and S. C. Cripps, "An efficient broadband reconfigurable power amplifier using active load modulation," *IEEE Microw. Wireless Compon. Lett.*, vol. 26, no. 6, pp. 443–445, Jun. 2016.
- [8] D. Vegas, M. Pampín, J. Perez-Cisneros, M. N. Ruiz, A. Mediavilla, and J. A. García, "Uhf class-e power amplifier design for wide range variable resistance operation," in *2018 IEEE/MTT-S International Microwave Symposium - IMS*, 2018, pp. 297–300.
- [9] M. Özen, K. Andersson, and C. Fager, "Symmetrical doherty power amplifier with extended efficiency range," *IEEE Transactions on Microwave Theory and Techniques*, vol. 64, no. 4, pp. 1273–1284, 2016.
- [10] D. A. Calvillo-Cortes, M. P. van der Heijden, M. Acar, M. de Langen, R. Wesson, F. van Rijs, and L. C. N. de Vreede, "A package-integrated chireix outphasing rf switch-mode high-power amplifier," *IEEE Transactions on Microwave Theory and Techniques*, vol. 61, no. 10, pp. 3721–3732, 2013.
- [11] P. H. Pednekar, W. Hallberg, C. Fager, and T. W. Barton, "Analysis and design of a doherty-like rf-input load modulated balanced amplifier," *IEEE Transactions on Microwave Theory and Techniques*, vol. 66, no. 12, pp. 5322–5335, 2018.
- [12] M. Özen and C. Fager, "Symmetrical doherty amplifier with high efficiency over large output power dynamic range," in *2014 IEEE MTT-S International Microwave Symposium (IMS2014)*, 2014, pp. 1–4.